

A Capillary Mixer with Adjustable Reaction Chamber Volume for Millisecond Time-Resolved Studies by Electrospray Mass Spectrometry

Derek J. Wilson and Lars Konermann*

Department of Chemistry, The University of Western Ontario, London, ON, N6A 5B7, Canada

A novel continuous-flow apparatus for on-line kinetic studies of (bio)chemical solution-phase processes by electrospray ionization mass spectrometry (ESI-MS) is described. The device is based on two concentric capillaries. Fluid is released from the inner capillary into the intercapillary space, where it mixes with solution flowing through the outer capillary, thus initiating the reaction of interest. Gas-phase analyte ions are formed near the tip of the outer capillary by pneumatically assisted ESI. This setup allows the mixer to be placed directly within the ion source, thus providing a minimal dead volume of ~8 nL. Time-resolved data can be recorded in both “spectral” and “kinetic” modes. In the former case, the position of the inner capillary is fixed at various points, such that entire mass spectra can be recorded for selected reaction times. For experiments in kinetic mode, the mass spectrometer monitors the signal intensity at selected m/z values, while the inner capillary is continuously pulled back, thus providing intensity–time profiles for specific reactive species. A theoretical framework is developed that allows the measured kinetics to be analyzed by taking into account the effects of laminar flow within the reaction capillary. Failure to take these effects into account results in erroneous rate constants. Studies on the demetalation kinetics of chlorophyll reveal that the apparatus can reliably measure rate constants up to at least 100 s^{-1} . This represents a substantial improvement over previous ESI-MS-based kinetic methods. Spectral mode experiments on the refolding of ubiquitin show the changing proportions of denatured and tightly folded protein subpopulations in solution. When monitored in kinetic mode, the refolding process was found to proceed with a rate constant of 5.2 s^{-1} .

Soon after the advent of electrospray ionization mass spectrometry (ESI-MS) in the late 1980s,^{1,2} it became clear that this technique has an enormous potential for kinetic studies on

solution-phase reactions.^{3,4} Following the initiation of a (bio)chemical process by mixing of two or more reactants, the kinetics can be monitored on-line, i.e., by direct injection of the reaction mixture into the ion source. The relative concentrations of multiple reactive species can be recorded as a function of time with extremely high sensitivity and selectivity. Transient intermediates may be identified based on their mass-to-charge ratio or their MS/MS characteristics. On-line ESI-MS kinetic studies have been carried out in a wide range of areas, including bioorganic chemistry,^{5,6} enzymology,^{7–11} protein folding and assembly,^{12,13} and isotope exchange experiments in the context of protein conformational dynamics.^{14–19}

The use of ionization techniques other than ESI for on-line kinetic MS studies has been explored by a number of groups.^{20–22} Due to its versatility, however, ESI-MS remains by far the most popular technique for studies of this kind. An alternative approach for kinetic measurements involves the use of quench–flow techniques in conjunction with off-line MS analysis.^{23,24} In quench–

- (3) Lee, E. D.; Mück, W.; Henion, J. D.; Covey, T. R. *J. Am. Chem. Soc.* **1989**, *111*, 4600–4604.
- (4) Konermann, L.; Douglas, D. J. *Methods Enzymol.* **2002**, *354*, 50–64.
- (5) Sam, J. W.; Tang, X. J.; Peisach, J. *J. Am. Chem. Soc.* **1994**, *116*, 5250–5256.
- (6) Bakhtiar, R.; Hop, C. E. C. A. *J. Phys. Org. Chem.* **1999**, *12*, 511–527.
- (7) Fligge, T. A.; Kast, J.; Bruns, K.; Przybylski, M. *J. Am. Soc. Mass Spectrom.* **1999**, *10*, 112–118.
- (8) Zechel, D. L.; Konermann, L.; Withers, S. G.; Douglas, D. J. *Biochemistry* **1998**, *37*, 7664–7669.
- (9) Northrop, D. B.; Simpson, F. B. *Bioorg. Med. Chem.* **1997**, *5*, 641–644.
- (10) Norris, A. J.; Whitelegge, J. P.; Faull, K. F.; Toyokuni, T. *Biochemistry* **2001**, *40*, 3774–3779.
- (11) Paiva, A. A.; Tilton, R. F.; Crooks, G. P.; Huang, L. Q.; Anderson, K. S. *Biochemistry* **1997**, *36*, 15472–15476.
- (12) Lee, V. W. S.; Chen, Y.-L.; Konermann, L. *Anal. Chem.* **1999**, *71*, 4154–4159.
- (13) Larson, J. L.; Ko, E.; Miranker, A. D. *Protein Sci.* **2000**, *9*, 427–431.
- (14) Katta, V.; Chait, B. T. *J. Am. Chem. Soc.* **1993**, *115*, 6317–6321.
- (15) Simmons, D. A.; Konermann, L. *Biochemistry* **2002**, *41*, 1906–1914.
- (16) Simmons, D. A.; Dunn, S. D.; Konermann, L. *Biochemistry* **2003**, *42*, 5896–5905.
- (17) Lin, H.; Dass, C. *Rapid Commun. Mass Spectrom.* **2001**, *15*, 2341–2346.
- (18) Maier, C. S.; Schimerlik, M. I.; Deinzer, M. L. *Biochemistry* **1999**, *38*, 1136–1143.
- (19) Eyles, S. J.; Dresch, T.; Gierasch, L. M.; Kaltashov, I. A. *J. Mass Spectrom.* **1999**, *34*, 1289–1295.
- (20) Brivio, M.; Fokkens, R. H.; Verboom, W.; Reinhoudt, D. N.; Tas, N. R.; Goedbloed, M.; van den Berg, A. *Anal. Chem.* **2002**, *74*, 3972–3976.
- (21) Ørsnes, H.; Graf, T.; Degn, H. *Anal. Chem.* **1998**, *70*, 4751–4754.
- (22) Northrop, D. B.; Simpson, F. B. *Arch. Biochem. Biophys.* **1998**, *352*, 288–292.
- (23) Miranker, A.; Robinson, C. V.; Radford, S. E.; Aplin, R.; Dobson, C. M. *Science* **1993**, *262*, 896–900.

* To whom correspondence should be addressed. E-mail: konerman@uwo.ca; <http://publish.uwo.ca/~konerman/>.

- (1) Bruins, A. P.; Covey, T. R.; Henion, J. D. *Anal. Chem.* **1987**, *59*, 2642–2646.
- (2) Fenn, J. B.; Mann, M.; Meng, C. K.; Wong, S. F.; Whitehouse, C. M. *Science* **1989**, *246*, 64–71.

flow experiments, the reaction is initiated by rapid mixing of the reactants, followed by mixing with a quenching agent, such as acid, base, or organic solvent, that abruptly stops the reaction after a specified period of time. An advantage of that technique is the possible incorporation of purification steps in situations where components of the reaction mixture would interfere with the MS analysis. Quench-flow methods undoubtedly represent a powerful tool for kinetic studies, but they can be problematic in cases where reactive species are not stable under the conditions of the quenched reaction mixture. Also, quench-flow studies are laborious because individual time points have to be measured in separate experiments.

Of particular importance for studies on a wide range of chemical and biochemical systems are techniques capable of providing kinetic data on rapid time scales, i.e., seconds to milliseconds or even microseconds.²⁵ On-line ESI-MS methods have been used for characterizing processes with half-lives down to roughly 30 ms.¹⁶ This temporal resolution is orders of magnitude lower than that obtainable in rapid-mixing experiments with optical detection.^{26,27} It therefore appears that there might still be considerable room for extending the time range that is accessible to MS-based kinetic techniques.

On-line kinetic studies can be carried out in two different modes of operation: (i) In "kinetic mode", the abundance of one or more ionic species is monitored as a function of time, e.g., by monitoring the intensity at selected m/z values on a quadrupole mass analyzer. This type of experiment provides detailed intensity-time profiles for individual reactive species, which allows the accurate determination of rate constants. Stopped-flow ESI-MS is a method capable of providing highly accurate data in kinetic mode.^{28,29} Unfortunately, this approach requires prior knowledge of the m/z value(s) of interest, thus posing a serious limitation for studies on processes that involve unknown intermediates. (ii) For experiments carried out in "spectral mode", entire mass spectra are recorded for selected reaction times, which allows the detection and identification of transient intermediates. The use of stopped-flow ESI-MS for studies in spectral mode is difficult, because entire mass spectra would have to be recorded on a millisecond time scale, which poses a challenge even for time-of-flight instruments or quadrupole ion traps. Experiments in spectral mode are more easily carried out by using continuous-flow methods. In contrast to stopped-flow ESI-MS, this approach does not involve real-time data acquisition; spectral mode data can therefore be recorded even with slow-scanning mass analyzers.^{5,12,15,30,31} Usually, the reaction chamber in continuous-flow studies is a capillary that is mounted between a mixer and the ESI source. The reaction time is determined by the capillary dimensions and by the solution flow rate. Controlling the reaction

time by changing the solution flow rate is not advisable because this may result in artifactual changes of analyte ion abundances.^{32,33} Reaction capillaries of different length are therefore most commonly used for recording spectra at different times points. A drawback of existing continuous-flow methods is the difficulty of obtaining intensity-time profiles of selected ions. These kinetic mode data have to be "pieced together" from multiple measurements carried out with different capillary lengths, in a manner analogous to quench-flow studies.

Up until now, different experimental methods had to be used for obtaining millisecond time-resolved MS data in kinetic and in spectral mode. The present study describes a continuous-flow mixer with adjustable reaction chamber volume that is capable of both modes of operation. Data can be recorded in kinetic mode by continually increasing the distance between the mixer and the ion source, while monitoring the abundance of selected ions. Alternatively, spectral mode experiments can be performed by choosing certain (fixed) reaction chamber volumes, such that entire mass spectra can be generated for selected time points. The temporal resolution of this system exceeds that of previous ESI-MS-based kinetic methods.

EXPERIMENTAL SECTION

Chemicals. Chlorophyll *a* from spinach and bovine ubiquitin were obtained from Sigma (St. Louis, MO). Distilled grade methanol and hydrochloric acid were supplied by Caledon (Georgetown, ON, Canada) and glacial acetic acid was supplied by BDH (Toronto, ON, Canada). All chemicals were used without further purification.

Optical Stopped-Flow Measurements. These measurements were performed on an SFM-4 instrument (Bio-Logic, Claix, France), using an observation wavelength of 664 nm for monitoring the demetalation of chlorophyll. The two stepper motor-driven syringes used were advanced at 3.5 mL/s each, for an instrument dead time of 3.3 ms. All experiments were carried out at room temperature (22 ± 1 °C).

On-Line Kinetic ESI-MS Measurements. These measurements were carried out using a custom-built continuous-flow mixing apparatus that is based on two concentric capillaries (Figure 1). The reaction of interest is initiated by mixing solutions from syringes 1 and 2 near the end of the inner capillary. The plungers of both syringes are advanced simultaneously and continuously by syringe pumps (Harvard Apparatus, model 22, Saint Laurent, PQ, Canada). The inner capillary consists of fused silica (100 ± 1.5 μm i.d., 167 ± 3 μm o.d., Polymicro Technologies, Phoenix, AZ). Its end is plugged by rapid curing, self-priming polyimide (HD Microsystems, Parlin, NJ). About 2 mm upstream from this plug, a ~ 80 μm deep notch is cut into the side of the inner capillary, which allows solution from syringe 1 to be expelled into the ~ 8 - μm -wide intercapillary space. The outer capillary consists of stainless steel (182 ± 2 μm i.d., 356 ± 6 μm o.d., Small Parts, Miami Lakes, FL) and has a length of 13 cm. The inner capillary passes through a three-way PEEK union (Upchurch Scientific, Oak Harbor, WA) and is directly connected to syringe 1. Within the PEEK union, a Flexon sleeve (Alltech, Deerfield,

(24) Houston, C. T.; Taylor, W. P.; Widlanski, T. S.; Reilly, J. P. *Anal. Chem.* **2000**, *72*, 3311–3319.

(25) Gruebele, M. *Annu. Rev. Phys. Chem.* **1999**, *50*, 485–516.

(26) Knight, J. B.; Vishwanath, A.; Brody, J. P.; Austin, R. H. *Phys. Rev. Lett.* **1998**, *80*, 3863–3866.

(27) Roder, H.; Shastry, M. C. R. *Curr. Opin. Struct. Biol.* **1999**, *9*, 620–626.

(28) Kolakowski, B. M.; Simmons, D. A.; Konermann, L. *Rapid Commun. Mass Spectrom.* **2000**, *14*, 772–776.

(29) Kolakowski, B. M.; Konermann, L. *Anal. Biochem.* **2001**, *292*, 107–114.

(30) Konermann, L.; Collings, B. A.; Douglas, D. J. *Biochemistry* **1997**, *36*, 5554–5559.

(31) Sogbein, O. O.; Simmons, D. A.; Konermann, L. *J. Am. Soc. Mass Spectrom.* **2000**, *11*, 312–319.

(32) Van Berkel, G. J.; Zhou, F.; Aronson, J. T. *Int. J. Mass Spectrom. Ion Processes* **1997**, *162*, 55–67.

(33) Konermann, L.; Silva, E. A.; Sogbein, O. F. *Anal. Chem.* **2001**, *73*, 4836–4844.

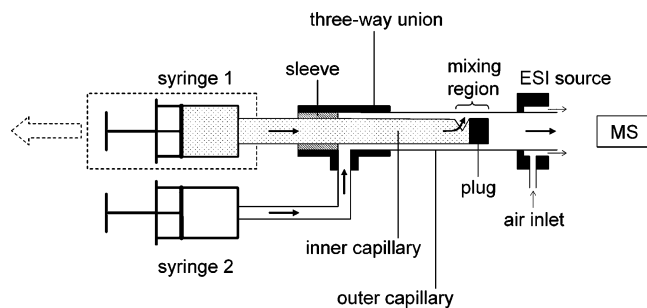


Figure 1. Schematic cross-sectional diagram of the experimental apparatus used in this study for time-resolved ESI-MS experiments. Syringes 1 and 2 deliver a continuous flow of reactants; mixing of the two solutions initiates the reaction of interest. The inner capillary can be automatically pulled back together with syringe 1 (as indicated by the dashed arrow), thus providing a means to control the average reaction time τ . Solid arrows indicate the directions of liquid flow. Small arrows in the electrospray (ESI) source region represent the directions of air flow. Further explanations are given in the text.

IL) around the inner capillary prevents leaking. The opposite end of the PEEK union is connected to the outer capillary, while its third port is connected to an inlet tube that delivers solution from syringe 2. This solution flows through the intercapillary space until it passes the mixer. The volume of the mixing region can be approximated as the $\sim 8\text{-}\mu\text{m}$ -wide and roughly 2-mm-long intercapillary space downstream of the notch, which corresponds to $\sim 8\text{ nL}$. For a total liquid flow rate of $60\ \mu\text{L}/\text{min}$, this results in a theoretical dead time (mixing time) of $\sim 8\text{ ms}$.

A 3-mm-long Delron block accommodates the end of the outer capillary. It has an inlet for compressed air and is designed to provide a collateral gas flow around the reaction mixture that exits from the capillary outlet. The high-voltage power supply of a triple quadrupole mass spectrometer (PE Sciex, API 365, Concord, ON, Canada) is connected directly to the outer capillary. This allows the production of gas-phase ions at the capillary outlet by pneumatically assisted ESI. Subsequently, these ions pass through the differentially pumped interface into the vacuum chamber of the mass spectrometer. The sprayer voltage was held at 6 kV.

For an average flow velocity \bar{v} in the reaction capillary, the (average) reaction time τ at the ion source is given by

$$\tau = l/\bar{v} \quad (1)$$

where l is the length of the reaction capillary, i.e., the distance between the mixer and the capillary outlet. In contrast to previous continuous-flow ESI-MS systems,^{5,16,30} l is variable for the setup used here; it can be controlled by changing the position of the inner capillary within the outer capillary. For a typical experiment, the mixer is initially located within the ESI source (i.e., at the end of the outer capillary), corresponding to $\tau \approx 0$. The inner capillary can be continuously pulled back together with syringe 1 by a stepper motor-controlled mechanism. Experiments can therefore be carried out in kinetic mode by monitoring the abundance of selected ions as a function of τ , typically with a dwell time of 30 ms. This mode of operation is possible because the Flexon sleeve within the three-way union provides a low enough friction to allow the continuous withdrawal of the inner capillary, while ensuring a leak-proof connection. A withdrawal rate corre-

sponding to $0.75\ \mu\text{L}/\text{min}$ was used for the experiments of this work. Control experiments confirmed that the baseline of the kinetic experiments is unaffected by the positioning of the inner capillary. Data in spectral mode are obtained for selected time points τ by monitoring the entire mass spectrum of the reaction mixture at fixed values of l .

For demetalation experiments, syringe 1 contained $40\ \mu\text{M}$ chlorophyll in methanol and syringe 2 contained HCl in methanol at concentrations ranging from 30 to 100 mM. Both syringes were advanced at $30\ \mu\text{L}/\text{min}$ for a total flow rate of $60\ \mu\text{L}/\text{min}$ in the reaction capillary. Ubiquitin refolding studies were carried out by having syringe 1 filled with $20\ \mu\text{M}$ protein in 46% water, 50% methanol, and 4% acetic acid. Syringe 2 contained water. The two syringes were advanced at 20 and $50\ \mu\text{L}/\text{min}$, respectively, for a total flow rate of $70\ \mu\text{L}/\text{min}$. Final solution conditions after mixing were 14.3% methanol and 1.1% acetic acid.

Safety Considerations. Like any experimental technique that is based on ESI-MS, the method described here involves the use of high electric potentials. Precautions should be taken to avoid contact with the outer capillary of the continuous-flow setup and with the components of the ion sampling interface of the mass spectrometer during operation. Syringes 1 and 2, and the syringe pumps used, should be properly grounded.

THEORY AND DATA ANALYSIS

The analysis of kinetic data obtained in continuous-flow experiments would be easiest in the hypothetical case of "plug flow", characterized by a constant flow velocity throughout the cross-sectional area of the reaction capillary. In this case, τ would be identical to the reaction time t . Traditional continuous-flow studies with optical detection are carried out under turbulent flow conditions, where constant mixing of fast and slow regions within the capillary effectively causes all analyte molecules to travel with a velocity close to \bar{v} . Data recorded under these conditions can be analyzed as if there were plug flow.^{34–37}

For on-line ESI-MS experiments, turbulent flow cannot normally be attained. This is due to the use of relatively narrow reaction capillaries, typically having an inner radius R of $100\ \mu\text{m}$ or less. Commonly used flow rates are in the range of tens to hundreds of microliters per minute, thus resulting in Reynolds numbers much smaller than the threshold value of 2000.³⁸ Under these conditions, the flow within the capillary is laminar, with a velocity profile $v(r)$ that is given by³⁹

$$v(r) = v_{\text{max}}(1 - (r^2/R^2)) \quad (2)$$

where r represents the radial position within the reaction capillary. The flow velocity at the center of the capillary, v_{max} , is twice the average flow velocity \bar{v} . This parabolic velocity profile has a tendency to distort the measured kinetics by "blurring" the time

(34) Fersht, A. *Structure and Mechanism in Protein Science*; W. H. Freeman & Co.: New York, 1999.

(35) Johnson, K. A. *Methods Enzymol.* **1995**, *249*, 38–61.

(36) Hartridge, H.; Roughton, F. J. W. *Proc. R. Soc. (London)* **1923**, *A104*, 376–394.

(37) Owens, G. D.; Margerum, D. W. *Anal. Chem.* **1980**, *52*, 91A–106A.

(38) Konermann, L. *J. Phys. Chem. A* **1999**, *103*, 7210–7216.

(39) Probstein, R. F. *Physicochemical Hydrodynamics*, 2nd ed.; John Wiley & Sons: New York, 1994.

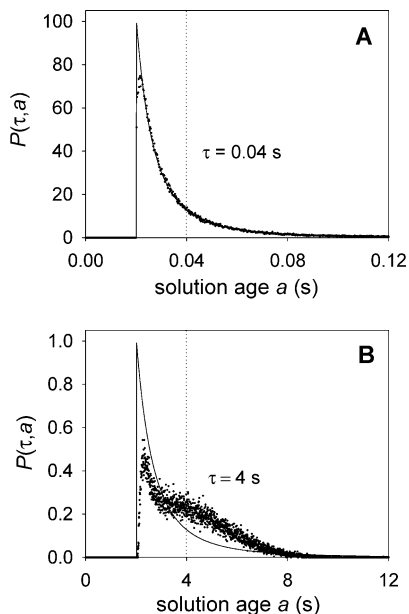


Figure 2. Age distribution functions $P(\tau, a)$ plotted vs solution age a for laminar flow. (A) Capillary length $l = 0.168$ cm, corresponding to an average reaction time of $\tau = 0.04$ s; (B) capillary length $l = 16.8$ cm, corresponding to $\tau = 4$ s. Solid lines are distribution functions calculated from eq 3, assuming a diffusion coefficient D of zero. The dotted curves are distribution functions simulated for $D = 5 \times 10^{-10}$ m²/s. The other parameters used are given in the text. Dotted vertical lines in both panels indicate $a = \tau$.

axis, because individual positions l along the reaction capillary *cannot* be associated with specific reaction times t . Instead, each value of l corresponds to a range of reaction times that are spread around the average value τ . We will now develop a data analysis strategy that takes into account these distortive laminar flow effects.

For analyte molecules traveling through the reaction capillary, the “age” a of each molecule is defined as the time required to move from the mixing point to the ion source. The probability that an analyte molecule has an age in the range $a \dots a + da$ is given by $P(\tau, a) da$, where $P(\tau, a)$ is the “age distribution function”. For laminar flow, $P(\tau, a)$ can be derived from eq 2; it is given by³⁸

$$P(\tau, a) = \frac{\tau^2}{2} \frac{1}{a^3} \quad \text{for } a \geq \tau/2$$

and

$$P(\tau, a) = 0 \quad \text{for } a < \tau/2 \quad (3)$$

As expected, this equation predicts an average solution age of $\langle a \rangle = \tau$ at the ion source. The solid lines in Figure 2 show examples of age distribution functions, calculated from eq 3, for $l = 0.168$ cm and for $l = 16.8$ cm (corresponding to $\tau = 0.04$ s and $\tau = 4$ s, respectively). The other parameters used for these calculated curves reflect the experimental conditions used in this work, i.e., a liquid flow rate of 65 $\mu\text{L}/\text{min}$, and a capillary radius of 91 μm , resulting in an average flow velocity of $\bar{v} = 0.042$ m/s. In the hypothetical case of plug flow, $P(\tau, a)$ would be a narrow peak (δ function) centered at $a = \tau$, as indicated by the dotted

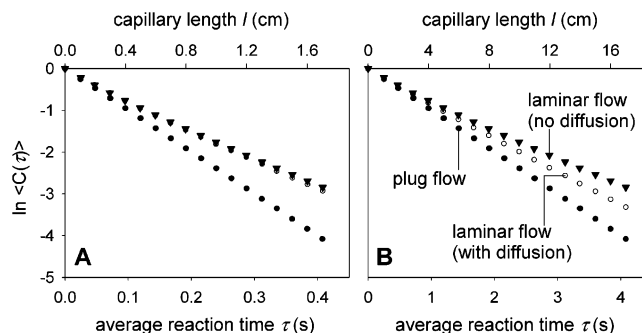


Figure 3. Simulated kinetic profiles for continuous-flow ESI-MS experiments. The natural logarithm of the signal intensity $\langle C(\tau) \rangle$ is plotted as a function of average reaction time τ for a first-order reaction with $C(t) = \exp(-k t)$. (A) $k = 10$ s⁻¹; (B) $k = 1$ s⁻¹. Both panels show three data sets, representing plug flow (solid circles), laminar flow without diffusion (solid triangles), and laminar flow with diffusion ($D = 5 \times 10^{-10}$ m²/s, open circles).

lines in Figure 2. This is in stark contrast to the distribution functions predicted by eq 4 that have their maximums at $a = \tau/2$.

Now consider a kinetic process for which the concentration of a particular reactive species as a function of time t is given by $C(t)$. Kinetic profiles monitored by the mass spectrometer represent an average concentration $\langle C(\tau) \rangle$ that can be calculated according to

$$\langle C(\tau) \rangle = \int_0^\infty C(a) P(\tau, a) da \quad (4)$$

This equation is valid for any age distribution function $P(\tau, a)$. For the laminar flow conditions considered here, substitution of eq 3 into eq 4 results in

$$\langle C(\tau) \rangle = \frac{\tau^2}{2} \int_{\tau/2}^\infty C(a) \frac{da}{a^3} \quad (5)$$

To illustrate the effects of laminar flow on the measured $\langle C(\tau) \rangle$ profiles we will consider the simple case of $C(t) = \exp(-k t)$. Kinetic profiles simulated based on eq 5 are shown as solid triangles in Figure 3 for $k = 10$ s⁻¹ (panel A) and $k = 1$ s⁻¹ (panel B). The logarithmic plots of these profiles have a roughly linear appearance with an average slope of $-0.698k$. Also shown are the corresponding kinetic profiles that would be expected in case of plug flow (solid circles in Figure 3), which have a slope of $-k$. A simple-minded “plug-flow analysis” of the kinetic data, assuming the reaction time t to be equal to the parameter τ , would therefore introduce an error of $\sim 30\%$ in the measured rate constants. For the current study, an iterative least-squares algorithm was therefore developed for fitting rate constants to the measured kinetic profiles based on eq 5. This approach can be employed for any mathematical $C(t)$ expression.

An important assumption made for the derivation of eq 5 was that the diffusion of analyte molecules within the reaction capillary is negligible. We will now explore under what conditions this approximation is justified. Diffusion continuously changes the radial position and, hence, the flow velocity $v(r)$ of individual analyte molecules as they travel along the reaction capillary. This diffusive mixing has a tendency to counteract the distortive effects

of laminar flow on the measured kinetics. Previous work has shown that laminar flow effects are virtually eliminated in the case of³⁸

$$\tau \gg R^2/36D \quad (6)$$

The dotted graphs in Figure 2 show simulated age distribution functions for laminar flow in the presence of diffusion. These $P(\tau, a)$ curves were calculated by using a numerical method,³⁸ assuming a diffusion coefficient of $D = 5 \times 10^{-10} \text{ m}^2 \text{ s}^{-1}$, which corresponds to a molecule the size of sucrose (this compound (MW 342) was chosen as an example to illustrate the behavior of a small biological molecule). The “noisy” appearance of the distributions in Figure 2 is due to the use of a random number generator for simulating the diffusion of individual analyte molecules. The effects of diffusion are insignificant for small values of τ , and the age distributions functions obtained under these conditions are very similar to those expected based on eq 3 (e.g., for $\tau = 0.04 \text{ s}$, Figure 2A). With increasing τ , more pronounced deviations between the two curves become apparent (e.g., for $\tau = 4 \text{ s}$, Figure 2B). In the limiting case described by relation 6, $P(\tau, a)$ resembles a Gaussian curve, centered at $a = \tau$ (data not shown).³⁸

The effects of analyte diffusion on the measured kinetics can be taken into account by using the appropriate simulated age distribution functions in eq 4. Diffusion is insignificant for rapid chemical processes that require short experimental time windows. As an example, Figure 3A shows that, for an exponential decay, $C(t) = \exp(-kt)$ with $k = 10 \text{ s}^{-1}$, virtually identical kinetic profiles are obtained for laminar flow in the presence of diffusion ($D = 5 \times 10^{-10} \text{ m}^2 \text{ s}^{-1}$, open circles) and in the absence of diffusion (solid triangles, calculated from eq 5). For slower processes that require longer experimental time windows, diffusion is no longer negligible. This is illustrated in Figure 3B for an exponential decay with $k = 1 \text{ s}^{-1}$. Generalizing the results obtained from these simulations, we conclude that diffusion does not have to be taken into account for processes that have essentially gone to completion within a time window of

$$\tau < R^2/36D \quad (7)$$

such that the analysis of kinetic data can be carried out based on eq 5. For $R = 91 \mu\text{m}$ and $D = 5 \times 10^{-10} \text{ m}^2 \text{ s}^{-1}$, the value of $R^2/36D$ equals 0.46 s, which roughly corresponds to the conditions of Figure 3A. Of course, this time window will be more extended for analytes with smaller diffusion coefficients. Equation 5 will also be valid for analyzing kinetic processes involving two reactants with different diffusion coefficients (e.g., the association of a protein with a small molecule), as long as condition 7 is satisfied for both species. However, if one of the two analytes is present in large excess, such that its concentration can be considered constant, only the diffusion coefficient of the limiting reactant will have to be taken into account.

RESULTS AND DISCUSSION

Instrument Performance in Kinetic Mode. The demetalation of chlorophyll *a* in acidic solution is a well-characterized process, during which the central magnesium of the porphyrin is

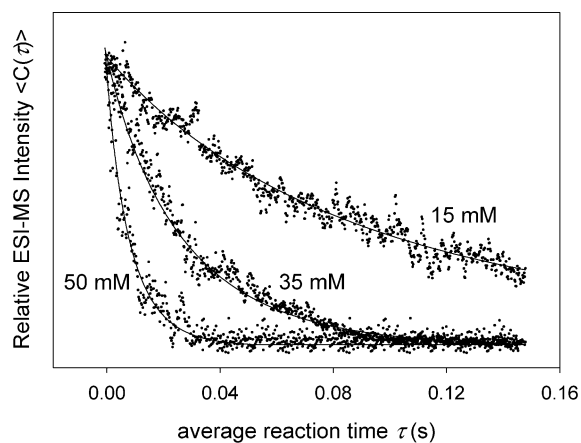


Figure 4. Demetalation kinetics of chlorophyll *a* (m/z 894) in methanol recorded by ESI-MS at three different concentrations of HCl. Solid line represent fits based on eq 5, with $C(t) = a \exp(-k_{\text{obs}}t)$.

displaced by two protons.^{40–42} This reaction represents a convenient test system, because it allows kinetic measurements by ESI-MS and by standard optical stopped-flow absorption spectroscopy. When studied under pseudo-first-order conditions, the rate constant of the reaction is given by $k_{\text{obs}} = k[\text{H}^+]^2$. The intrinsic rate constant k in this expression is known to be strongly solvent-dependent.^{41,42}

The apparatus depicted in Figure 1 was used for monitoring the kinetics of chlorophyll demetalation in methanol solution for acid concentrations ranging from 15 to 50 mM. Figure 4 depicts three representative kinetic profiles, obtained by monitoring the intensity of singly charged chlorophyll at m/z 894. Also shown are fits to the experimental data based on eq 5, with $C(t) = a \exp(-k_{\text{obs}}t)$. The pseudo-first-order rate constants k_{obs} obtained by ESI-MS were plotted as a function of acid concentration (Figure 5, solid triangles). The open circles in Figure 5 represent k_{obs} values obtained from control experiments carried out by optical stopped-flow spectroscopy. There is excellent agreement between these two data sets throughout the whole range, covering pseudo-first-order rate constants from about 10 to 100 s^{-1} . The use of higher acid concentrations to obtain even larger rate constants was not possible due to the onset of corona discharge in the ion source region. Nevertheless, it is clear that the temporal resolution of our novel mixing device exceeds that of other on-line ESI-MS techniques, which so far allowed rate constants up to $\sim 25 \text{ s}^{-1}$ to be measured.¹⁶

The solid line in Figure 5 represents a quadratic fit to the k_{obs} values measured by ESI-MS, based on the expression $k_{\text{obs}} = k[\text{H}^+]^2$. The resulting intrinsic rate constant has a value of $k = 0.048 \pm 0.002 \text{ mM}^{-2} \text{ s}^{-1}$. Within experimental error, this is identical to the k value of $0.050 \pm 0.001 \text{ mM}^{-2} \text{ s}^{-1}$ that was obtained through a quadratic fit to the corresponding optical data (fit not shown). The k_{obs} values obtained for acid concentrations of 45 and 50 mM evidently deviate from the expected quadratic behavior; therefore, these data points were not included for the fitting procedure. This deviation is likely due to a change in

(40) Heaton, J. W.; Lencki, R. W.; Marangoni, A. G. *J. Agric. Food. Chem.* **1996**, *44*, 399–402.

(41) Berezin, D. B.; Drobysheva, A. N.; Karmanova, L. P. *Russ. J. Phys. Chem.* **1976**, *50*, 720–723.

(42) Mazaki, H.; Watanabe, T. *Bull. Chem. Soc. Jpn.* **1988**, *61*, 2969–2970.

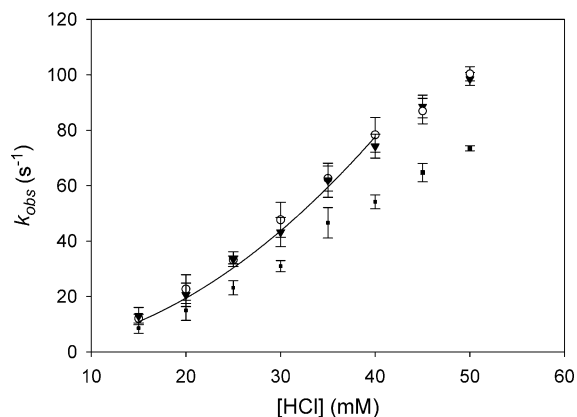


Figure 5. Pseudo-first-order rate constants k_{obs} for the demetalation of chlorophyll *a* as a function of HCl concentration. Solid triangles are the results of ESI-MS kinetics that were analyzed based on eq 5, taking into account laminar flow effects. The solid line is a quadratic fit to these data (k_{obs} values measured for the two highest acid concentrations were not considered for the fit). Open circles are data measured by standard optical stopped-flow spectroscopy. Also shown are k_{obs} values that were obtained from the ESI-MS data by using a "plug-flow" data analysis that fails to take into account laminar flow effects (small solid squares). Error bars are standard deviations, based on at least four independent measurements for each acid concentration.

reaction mechanism which has previously been found to take place at high acid concentrations.⁴¹

Figure 5 also shows the values of k_{obs} that are obtained from an analysis that neglects the laminar flow profile within the reaction capillary ("plug-flow analysis", solid squares). In this case, the measured kinetics were assumed to have the form $\langle C(\tau) \rangle = \exp(k_{\text{obs}}\tau)$, with $\tau = l/\bar{v}$, as defined above. The rate constants determined by this method are lower than the actual values by a factor of 0.69 ± 0.03 , which is in excellent agreement with the value of 0.689 that is expected based on the results of the Theory and Data Analysis section. These observations confirm that laminar flow effects have to be taken into account for the accurate determination of rate constants under the conditions of the current work, and they attest to the validity of eq 5 as a data analysis tool.

Protein Folding Monitored in Spectral and Kinetic Modes.

ESI-MS has become a standard method for monitoring conformational changes of proteins. In the positive ion mode, gas-phase proteins generated from tightly folded solution-phase conformations typically show relatively low charge states. In contrast, ions formed from unfolded proteins are more highly protonated and show a wider charge-state distribution. The physical reasons underlying this relationship between solution-phase protein conformation and ESI charge-state distribution are still a matter of debate.^{43–47} Ubiquitin is a small (8565 Da) protein that is commonly used as a model system for folding studies.^{48,49} Its compact native

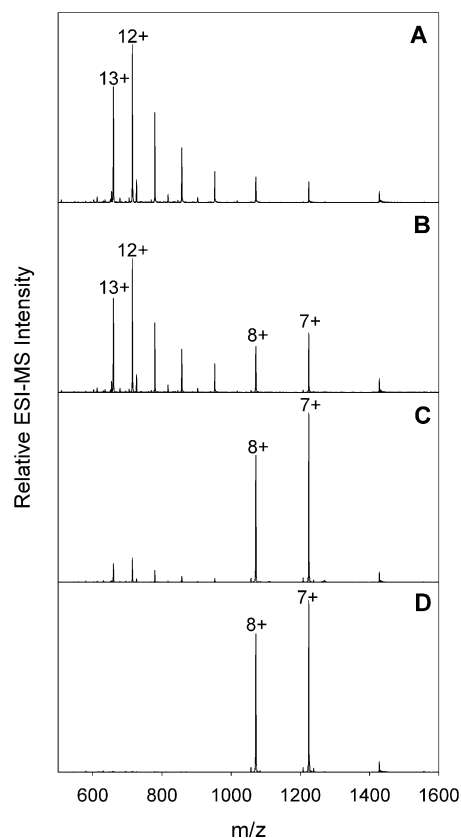


Figure 6. Refolding of ubiquitin studied in spectral mode. ESI mass spectra are depicted for average reaction times of (A) $\tau \approx 0$, (B) $\tau = 160$ ms, and (C) $\tau = 2.1$ s. The spectrum shown in panel D was recorded 5 min after initiation of refolding in a manual mixing experiment with off-line analysis. Notation: 13+ represents protein ions [ubiquitin + 13H]¹³⁺, etc. Panels A–C also show some minor peaks that presumably correspond to fragmentation products of the more highly charged protein ions.

structure breaks down in acidic solutions containing organic cosolvents such as methanol, to form an extended "A state" that has a non-native α -helical structure.⁵⁰ Folding transitions involving the A state of ubiquitin have previously been studied by ESI-MS, albeit not in kinetic experiments.^{14,51}

Here, the refolding of ubiquitin is used as a test reaction to demonstrate the performance of our continuous-flow setup in kinetic and in spectral mode. The A state was populated by exposing the protein to 50% methanol and 4% acetic acid; refolding was initiated by mixing with an excess volume of water (see Experimental Section). ESI mass spectra of ubiquitin for different times after initiation of refolding are depicted in Figure 6. The initial spectrum, recorded for $\tau \approx 0$ ms (Figure 6A), shows the 13+ and 12+ charge states as the ions with the highest abundances. This spectrum is practically indistinguishable from that of the protein prior to initiation of refolding (data not shown) and very similar to ubiquitin A state spectra that have been published previously.^{14,51} As refolding proceeds, the relative abundance of highly charged protein ions decreases and that of

(43) Chowdhury, S. K.; Katta, V.; Chait, B. T. *J. Am. Chem. Soc.* **1990**, *112*, 9012–9013.

(44) Fenn, J. B. *J. Am. Soc. Mass Spectrom.* **1993**, *4*, 524–535.

(45) Konermann, L.; Rosell, F. I.; Mauk, A. G.; Douglas, D. J. *Biochemistry* **1997**, *36*, 6448–6454.

(46) Kaltashov, I. A.; Eyles, S. J. *Mass Spectrom. Rev.* **2002**, *21*, 37–71.

(47) Grandori, R. *J. Mass Spectrom.* **2003**, *38*, 11–15.

(48) Vijay-Kumar, S.; Bugg, C. E.; Cook, W. J. *J. Mol. Biol.* **1987**, *194*, 531–544.

(49) Kakuta, M.; Jayawickrama, D. A.; Wolters, A. M.; Manz, A.; Sweedler, J. V. *Anal. Chem.* **2003**, *75*, 956–960.

(50) Brutscher, B.; Brunschweiler, R.; Ernst, R. R. *Biochemistry* **1997**, *36*, 6.

(51) Konermann, L.; Douglas, D. J. *J. Am. Soc. Mass Spectrom.* **1998**, *9*, 1248–1254.

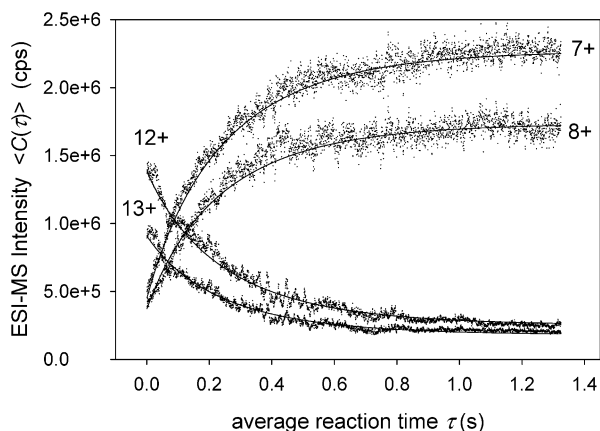


Figure 7. Refolding of ubiquitin studied in kinetic mode for four selected protein ions. Solid lines are fits based on eq 5.

the 8+ and 7+ ions increases (Figure 6B,C). The final spectrum was recorded off-line 5 min after initiation of refolding in a manual mixing experiment. It shows the 8+ and 7+ ions as the only dominant peaks, indicating that virtually all of the proteins have refolded into a compact conformation (Figure 6D).

Figure 7 shows data measured in kinetic mode, obtained by recording the abundance of 13+, 12+, 9+, and 8+ ions as a function of the average reaction time τ . The diffusion coefficient of ubiquitin can be estimated to be around $D = 1 \times 10^{-10} \text{ m}^2/\text{s}$.⁵² According to condition 7, this implies that diffusion effects on the observed kinetics are negligible in an experimental time window up to $\tau \approx 2 \text{ s}$. The data can therefore be fitted based on eq 5 (solid lines in Figure 7). $\langle C(\tau) \rangle$ expressions for the 13+ and 12+ ions were generated by assuming the model function $C(t) = a_1 \exp(-k_{\text{obs}}t) + a_0$, whereas the analysis of the 8+ and 7+ ions was based on $C(t) = b_1(1 - \exp(-k_{\text{obs}}t)) + b_0$. The use of an offset in the exponential decays takes into account the observation that refolding does not go to completion within the experimental time window of $\sim 1.3 \text{ s}$. Instead, the kinetic profiles level off at $\sim 20\%$ of their initial values. This effect can be attributed to a subpopulation of slow-folding ubiquitin molecules that contain non-native *cis*-proline isomers.⁵³ Proline isomerization, taking place on the order of tens of seconds,⁵⁴ is the rate-limiting step for the refolding of this subpopulation. Figure 6D indicates that after 5 min these slow-folding proteins have also attained a compact conformation. Processes occurring on such a slow time scale are beyond the range accessible by our rapid mixing setup.

The k_{obs} values obtained from the four fits in Figure 7 are in close agreement: 5.3 (8+), 5.3 (9+), 5.2 (12+), and 5.1 s^{-1} (13+), for an average value of 5.2 s^{-1} . Evidently, the experimental kinetics are well described by these monoexponential fits. This is in line

with previous work that has shown ubiquitin to be a two-state folder, except for those few protein molecules that are affected by proline isomerization.⁵³ Unfortunately, a direct comparison of our measured k_{obs} values with refolding rate constants from the literature is not possible, because previous kinetic studies involved the use of chemical denaturants that are not easily compatible with ESI-MS. Also, it is noted that wild-type ubiquitin does not contain any tryptophan residues or other chromophores that could serve as optical probes in kinetic refolding experiments. Previous kinetic studies were therefore carried out on a recombinant protein variant that contained a non-native tryptophan.^{53,55,56} Because chromophores are not required for the ESI-MS-based approach used here, kinetic studies could be performed directly on the wild-type protein.

CONCLUSIONS

We have developed a novel method for millisecond time-resolved studies by ESI-MS. The reaction volume of the described capillary mixing device is adjustable and can be controlled automatically. In contrast, previously available continuous-flow methods involved the use of reaction capillaries with different (fixed) lengths for controlling the reaction time, which caused the kinetic experiments to be relatively laborious.^{30,45} Also, the reproducible positioning of each of the reaction capillaries within the ion source represents a potential problem with this earlier approach. The method described in the current study eliminates both of these difficulties. Our novel mixing device offers the unique advantage of allowing ESI-MS-based experiments in two modes of operation; in "spectral mode", entire mass spectra can be recorded for selected time points, and in "kinetic mode", the intensity of selected ion signals can be monitored as a function of the average reaction time τ . The device allows first-order rate constants up to at least 100 s^{-1} to be measured reliably, which represents an improvement over previous time-resolved ESI-MS methods by at least a factor of 4. A potential concern for experiments on this time scale is the mixing efficiency of the reactant solutions in the intercapillary space. However, even the highest rate constants measured by ESI-MS in this work are in excellent agreement with the results of control experiments carried out on a standard commercial stopped-flow instrument, thus indicating that the mixing efficiency is not a limiting factor. In summary, it appears that the described method represents a versatile novel tool for kineticists working in a wide range of different areas, including enzymology, protein folding, and physical organic chemistry.

ACKNOWLEDGMENT

Financial support for this work was provided by the Natural Sciences and Engineering Research Council of Canada (NSERC), the Canada Foundation for Innovation (CFI), and the Provincial Government of Ontario.

Received for review June 22, 2003. Accepted September 10, 2003.

AC0346757

(52) Clark, S. M.; Konermann, L. *J. Am. Soc. Mass Spectrom.* **2003**, *14*, 430–441.

(53) Krantz, B. A.; Sosnick, T. R. *Biochemistry* **2000**, *39*, 11696–11701.

(54) Brandts, J. F.; Brennan, M.; Lin, L. *Proc. Natl. Acad. Sci. U.S.A.* **1977**, *74*, 4178–4181.

(55) Khorasanizadeh, S.; Peters, I. D.; Butt, T. R.; Roder, H. *Biochemistry* **1993**, *32*, 7054–7063.

(56) Khorasanizadeh, S.; Peters, I. D.; Roder, H. *Nat. Struct. Biol.* **1996**, *3*, 193–205.